Supporting Information for

Electronic Modulation of NiO by Constructing Amorphous/Crystalline Heterophase to Improve Photocatalytic Hydrogen Evolution

Linke Cai[a†], Bo Yan[a†], Qian Xue[b†], Jiling Li[a], Pu Liu[a], Xueqiang Qi[b*] & Guowei Yang[a*]

[a] State Key Laboratory of Optoelectronic Materials and Technologies, Nanotechnology Research Center, School of Materials Science & Engineering, Sun Yat-sen University, Guangzhou 510275, P. R. China

[b] School of Chemistry and Chemical Engineering, Chongqing University of Technology, Chongqing 400054, China

[†] These authors contributed equally to this work.

[*] Corresponding authors: xqqi@cqut.edu.cn, stsygw@mail.sysu.edu.cn

Table S1. Mass fraction of Ni in NiO_x-CN samples with different NiO-LAL content.

Samples	**NiO_2-CN**	**NiO_4-CN**	**NiO_6-CN**	**NiO_8-CN**
Mass fraction of Ni	8.75%	17.13%	19.03%	24.13%

Table S2. BET surface areas of g-C_3N_4, NiO-LAL and NiOx-CN samples with different NiO-LAL content.

Samples	**g-C_3N_4**	**NiO_2-CN**	**NiO_4-CN**	**NiO_6-CN**	**NiO_8-CN**	**NiO-LAL**
BET Surface Area ($m^2 \cdot g^{-1}$)	199.87	90.10	100.31	92.72	84.86	4.48

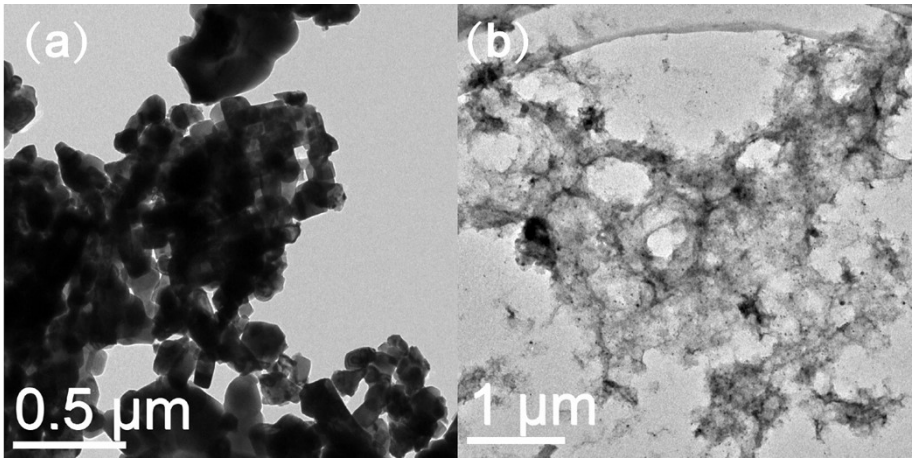

Figure S1. TEM images of NiO before laser treatment (a) and NiO-LAL at low magnification (b).

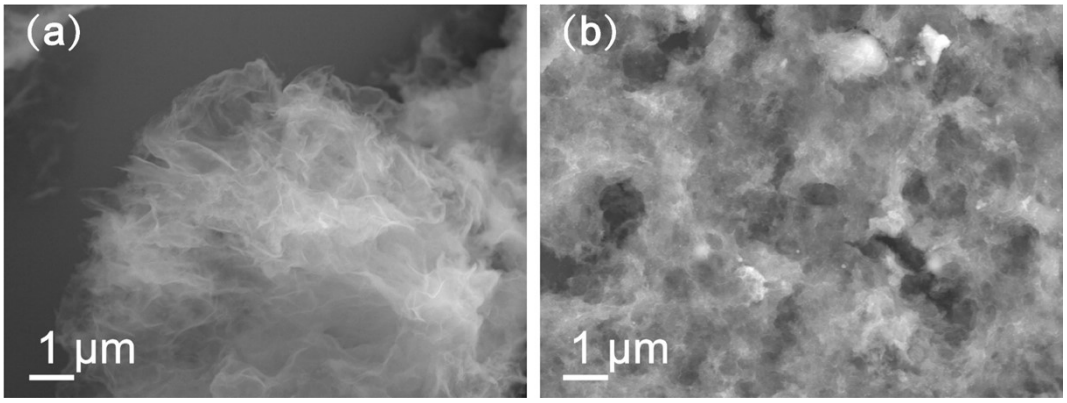

Figure S2. SEM images of g-C_3N_4 (a) and NiO-LAL (b).

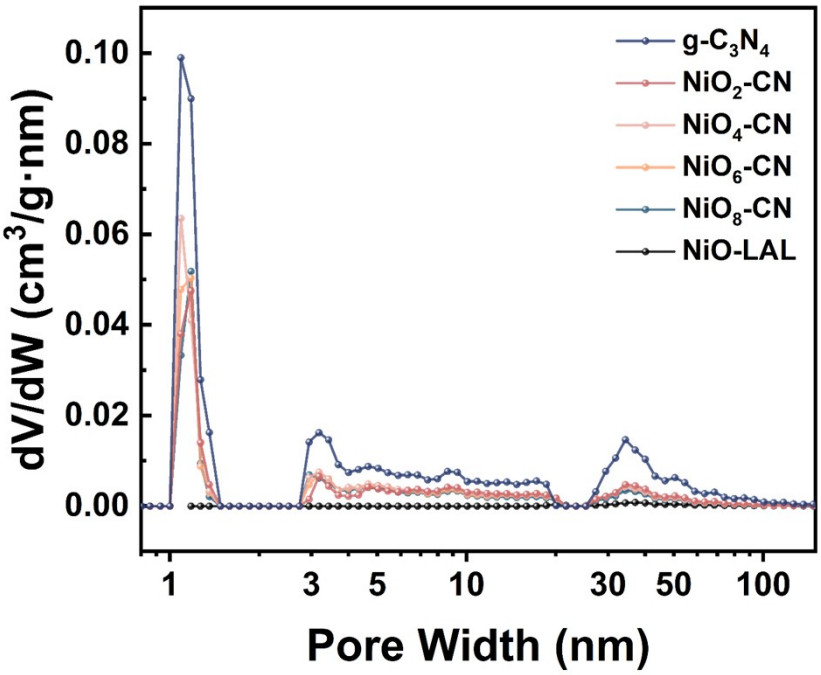

Figure S3. DFT pore volume distributions of as-prepared samples.

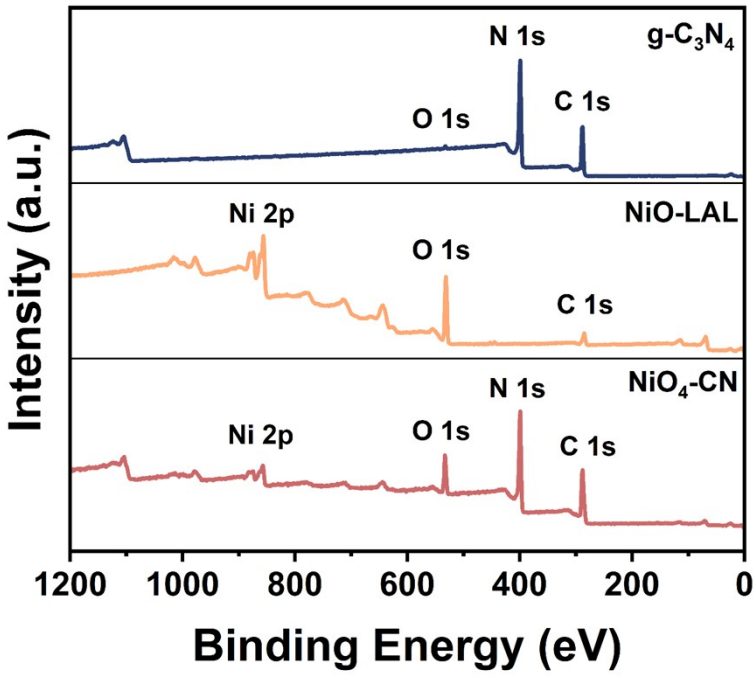

Figure S4. XPS spectra of the survey for g-C_3N_4, NiO-LAL and NiO_4-CN.

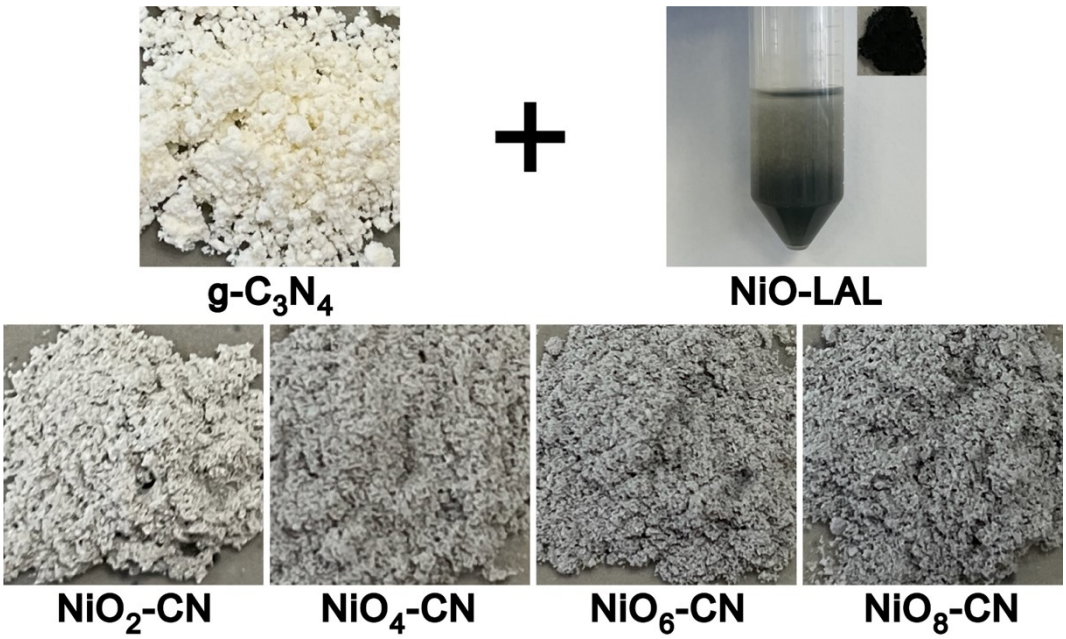

Figure S5. Photographs of g-C_3N_4, NiO-LAL and NiO_x-CN samples with different NiO-LAL content.

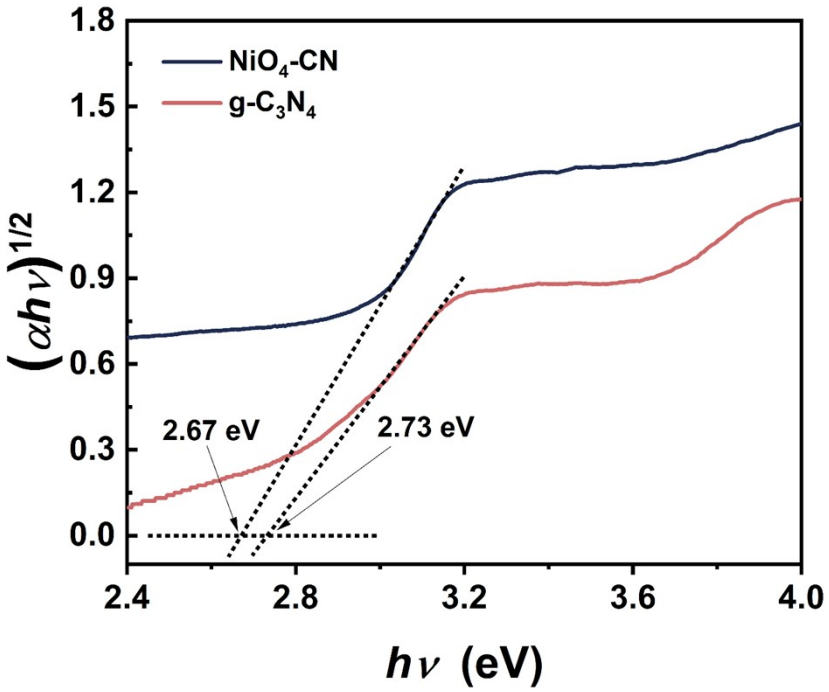

Figure S6. The plots of $(\alpha h\nu)^{1/2}$ versus $h\nu$ for the band energies of g-C_3N_4 and NiO_4-CN.

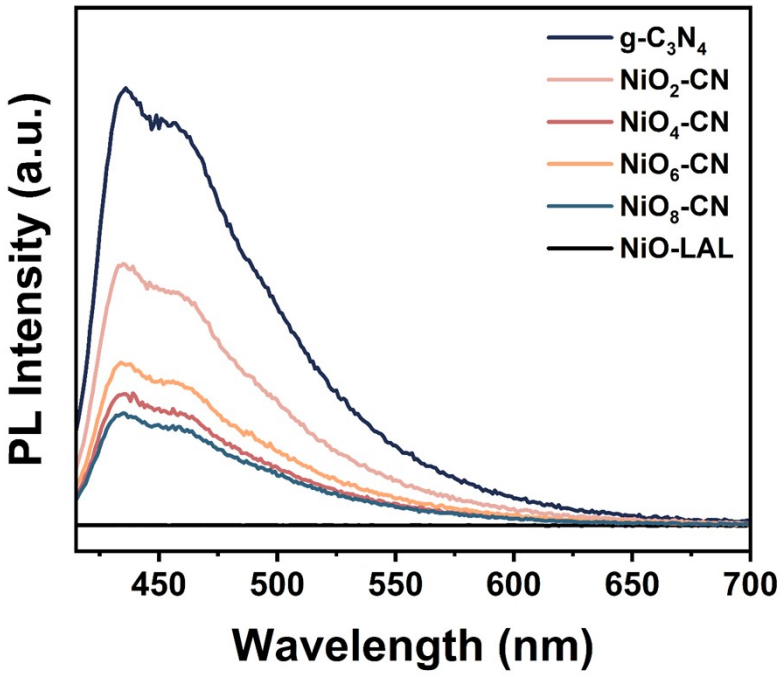

Figure S7. PL spectroscopy of g-C_3N_4, NiO-LAL and NiO_x-CN samples with different NiO-LAL content.

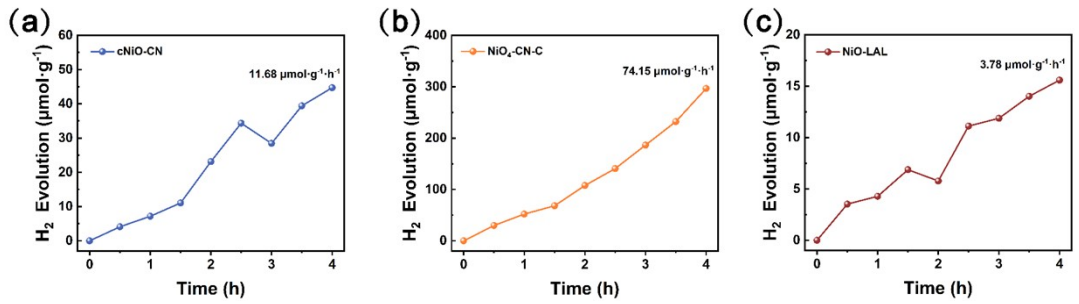

Figure S8. Photocatalytic H_2 generation performances of cNiO-CN (a), NiO_4-CN-C (b) and NiO-LAL (c).

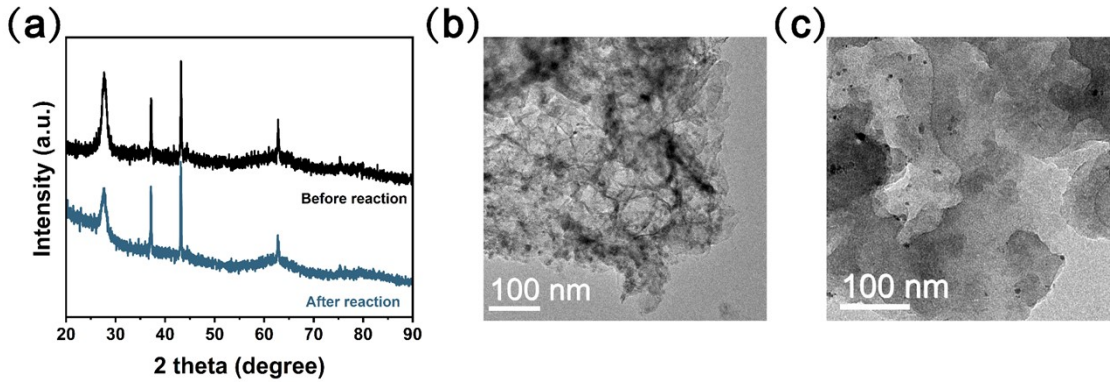

Figure S9. XRD patterns of NiO_4-CN before and after photocatalytic reaction (a), and TEM images of NiO_4-CN before (b) and after (c) photocatalytic reaction.

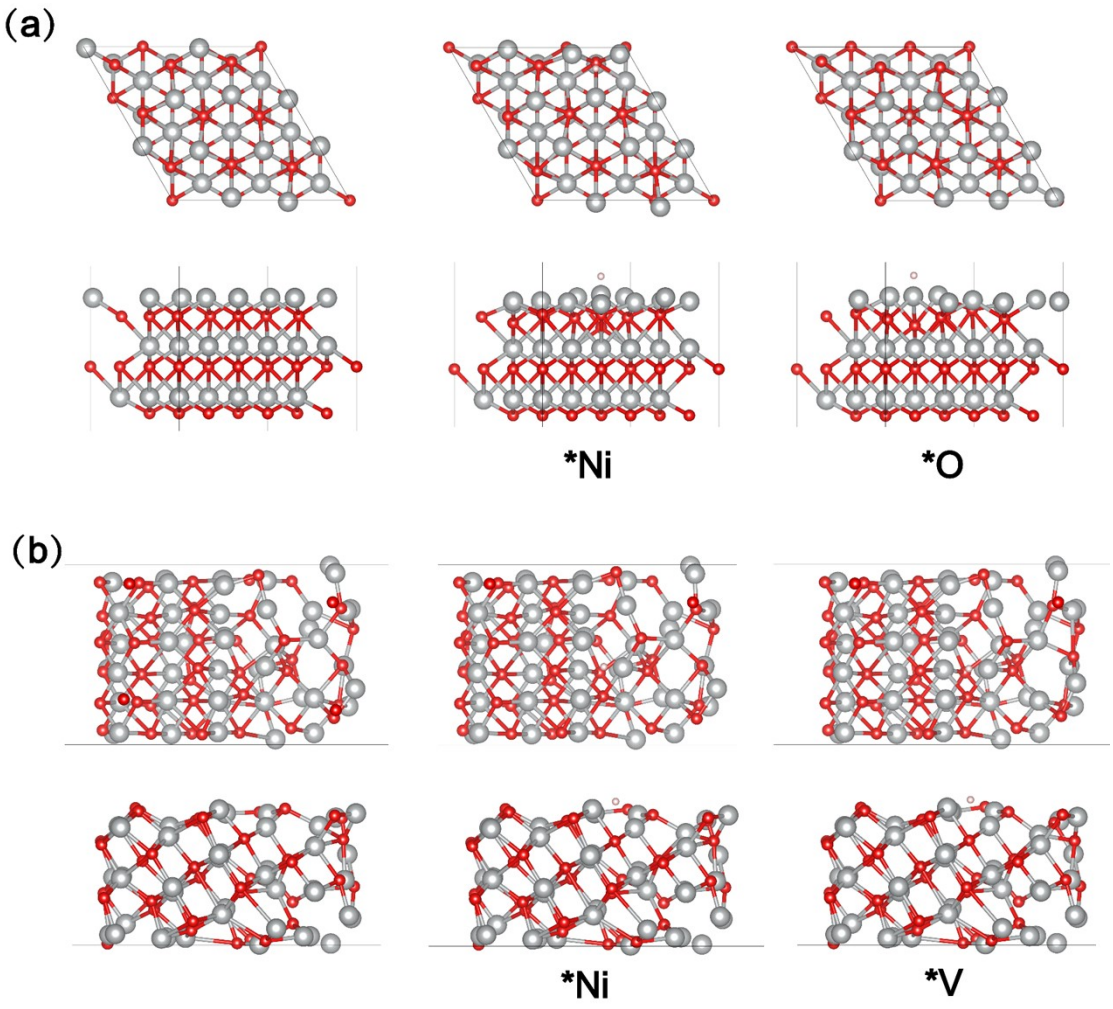

Figure S10. The structural models of pristine NiO (a) and amorphous/crystalline NiO homojunction (b).

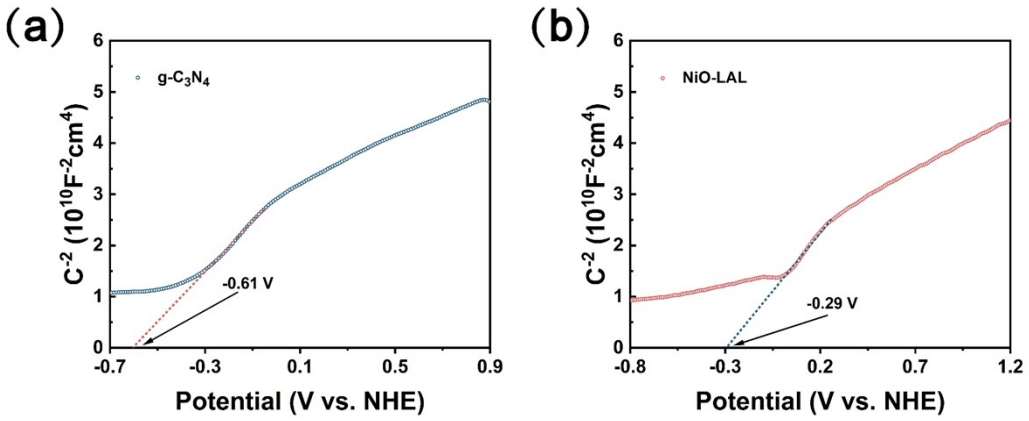

Figure S11. The Mott-Schottky plots of g-C_3N_4 (a) and NiO-LAL (b).